Learning evolution design of multiband-transmission fiber Bragg grating filters

Su-Frang Shu
Yinchieh Lai
Ci-Ling Pan, MEMBER SPIE
National Chiao Tung University
Institute of Electro-Optical Engineering
Hsinchu 300, Taiwan
E-mail: sfshu@mail.cyit.edu.tw

Abstract. A composite fiber Bragg grating (FBG) structure with several apodized sections is utilized for designing dense wavelength division multiplexing (DWDM) multiband transmission filters. A learning genetic algorithm (LGA) is also developed to determine the optimum design parameters of these filters. By taking advantage of a knowledge base (KB) that stores the FBG parameter sets and the corresponding transmission profile feature sets, our LGA can generate a suitable initial population and perform evolutionary optimization starting from it. This has made the LGA evolve more quickly to more accurate results than the methods without using the KB. The LGA can also store new results into the KB according to its decision procedure and improve its precision of initial prediction as it works through more and more examples. [DOI: 10.1117/1.1602087]

Subject terms: artificial intelligence; genetic algorithm; fiber Bragg grating; optical fiber filter; wavelength division multiplexing.

Paper 030029 received Jan. 16, 2003; revised manuscript received May 13, 2003; accepted for publication May 27, 2003.

1 Introduction

One of the focused efforts for dense wavelength division multiplexing (DWDM) technology development is the possibility of achieving denser wavelength channels and lower crosstalks among adjacent channels. As a DWDM add-drop device, a filter made of a fiber Bragg grating (FBG) is typically designed to provide high reflection in the reflection band and low sidelobe loss outside the band.[1,2] The advantages of using FBG filters mainly come from the fact that their reflection profile can be selectively designed and the bandwidth can be narrower than other types of filters.[3] Changing the profile sharpness and the sidelobe characteristics is typically achieved by applying suitable apodization on the refractive index modulation profile of the FBG. Because of this, determining the optimized apodization shape becomes an important issue for actually fabricating high performance FBG filters.[4]

In the literature, there are some developments for FBG inverse-design synthesis, including the Gel'fand-Levitan-Marchenko (GLM) integral equations used for both the exact solutions in Ref. 5 and the iterative solutions in Ref. 6, the Fourier transform techniques in Ref. 7, and the binary-coded genetic algorithm (GA) in Ref. 8. The real-coded GA work in Ref. 9 as an inverse-design tool is used to generate the optimized FBG parameters that can produce stop bands with steep edges and low sidelobes.[9] Based on the theoretical model in Ref. 10, Ref. 9 used several apodized sections of uniform FBGs with a constant period Λ to realize a single-band filter. In the present work, the FBG structure in Ref. 9 is extended to a composite structure with several cascading units that have a pitch period difference $\Delta\Lambda$ between adjacent units. Moreover, a learning genetic algorithm (LGA) is developed by utilizing a knowledge base (KB) that stores pairs of the FBG parameter set (including the unit-length L and the refractive index modulation depth δn) and the FBG transmission profile feature set (including the depth of stop band D and the stop-band widths $B1$, $B2$, and $B3$ as shown in Fig. 1). Here the depth of stop band D represents the transmission loss in decibels within the stop band. The stop-band widths $B1$, $B2$, and $B3$ are the widths of the stop band at 0.1, 0.5, and 0.9 total depth, respectively. The central wavelength of the first stop band is determined by the grating period Λ, and the wavelength difference between two adjacent stop bands is determined by the grating period difference $\Delta\Lambda$. These two parameters are determined at the first step when the retrieving procedure starts. At the evolutionary optimization stage, they are combined with the parameter set from the KB to form a seed parameter set. This seed is then applied with some perturbations to generate a suitable initial population for starting the LGA.

2 Structure of the Knowledge Base

2.1 *Modeling of Composite FBGs*

Figure 2 shows the composite FBG structure used in the present work. The apodized function as a function of the section index i has a form, as shown in Eq. (1).

$$A(i) = 1/2\{\cos^2[\pi(i-1-0.5N_s)/N_s] + \cos^2[\pi(i-0.5N_s)/N_s]\}. \quad (1)$$

Here N_s is the total number of sections in a unit. The transmission matrix of a FBG unit with N_s sections can be calculated by multiplying the N_s transmission matrices of the unit. Let the unit length be L. The arbitrary i'th section has the length l_i, and

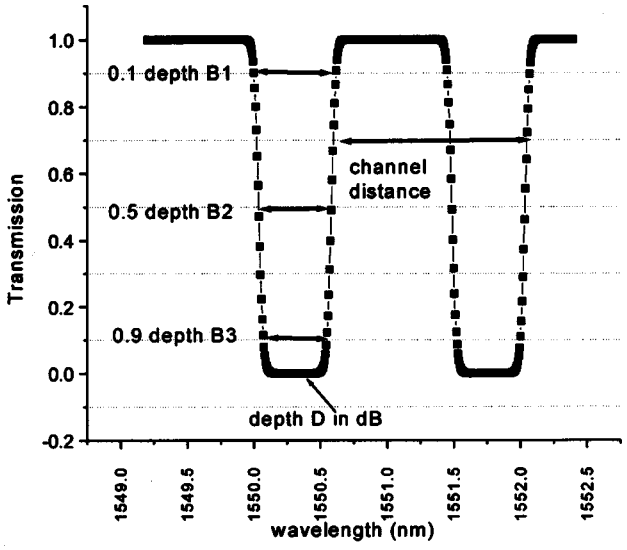

Fig. 1 The feature parameters of a spectrum.

$$L=\sum_{i=1}^{N_s} l_i .$$

The net transmission matrix of the whole unit can be represented as shown in Eq. (2).

$$[T]=[Tl_1][Tl_2][Tl_3]\ldots[Tl_i]\ldots[Tl_{Ns}]. \tag{2}$$

If k units are lined up together to form a FBG fiber with the total length kL, then the total transmission matrix $[T]_{\text{total}}$ will be the product of all unit transmission matrices as shown in Eq. (3).

$$\begin{bmatrix} a(0) \\ b(0) \end{bmatrix} = \begin{bmatrix} T_{11} & T_{12} \\ T_{21} & T_{22} \end{bmatrix} \begin{bmatrix} a(kL) \\ b(kL) \end{bmatrix}. \tag{3}$$

The transmission $T(\lambda)$ as a function of the wavelength can be calculated according to Eq. (4).

$$T(\lambda)=1/|T_{11}|^2. \tag{4}$$

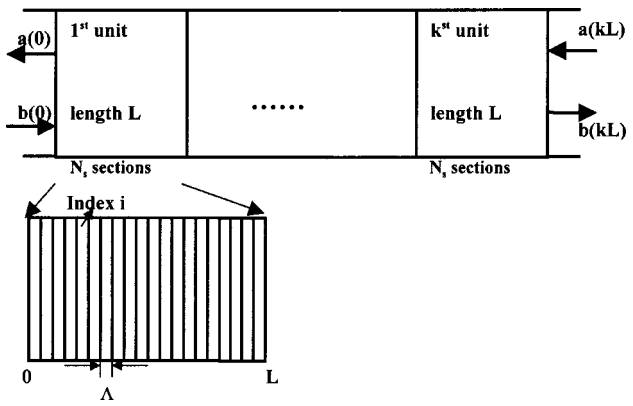

Fig. 2 The composite FBG structure consists of k units with N_s sections of uniform gratings in each unit.

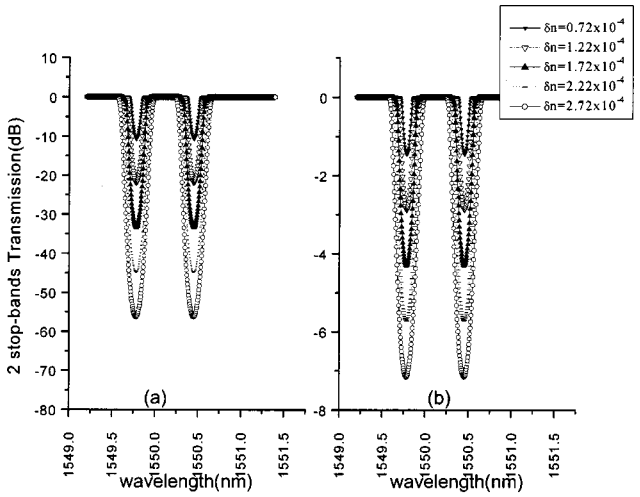

Fig. 3 The influence of the unit length L and the modulation depth δn on the transmission spectra: (a) $L=2.04$ and (b) $L=2.54$ cm.

2.2 *Influences of Length L and Modulation Depth δn on the Transmission Profiles*

We can get a transmission profile from a parameter set $(L,\delta n)$, and thus by variating δn and L we can construct a series of profiles. The transmission profiles plotted in Fig. 3(a) are calculated with the same parameters listed in Table 1, except that the refraction index modulation depth δn is set to be 0.72×10^{-4}, 1.22×10^{-4}, 1.72×10^{-4}, 2.22×10^{-4}, and 2.72×10^{-4}, respectively, from the inside to the outside profiles. The right-hand side profiles in Fig. 3(b) have the same parameters as the left-hand side profiles, except with a larger FBG length L. The increased FBG length deepens the stop bands as a larger refractive index will also do. This graph shows how the transmission features of the filters will depend on L and δn. The knowledge base will use these two parameters as a characteristic set to store various kinds of filter profile features.

2.3 *Formation of the Knowledge Base*

Figure 4 is drawn by calculating 100 parameter sets in the form of $(L,\delta n)$ to get the corresponding feature sets in the form of $(D,B1,B2,B3)$. The LGA uses these parameter sets and the corresponding feature sets as part of the KB. The relationship between the profile features and the parameters $(L,\delta n)$ can be seen clearly from Fig. 4. Here the top-left plot is for feature D, the top-right for feature $B1$, the bottom-left for feature $B2$, and the bottom-right for feature $B3$. After the KB is set up offline, the target spectrum can be compared with these sets before evolution to form a suitable initial population for the LGA.

Table 1 Parameter sets for the two channel transmission profiles in Fig. 3.

Parameters	L(cm)	Λ(nm)	δn	$\Delta\Lambda$(nm)
Fig. 3(a)	2.04	534	1.22×10^{-4}	0.231
Fig. 3(b)	2.54	534	1.22×10^{-4}	0.231

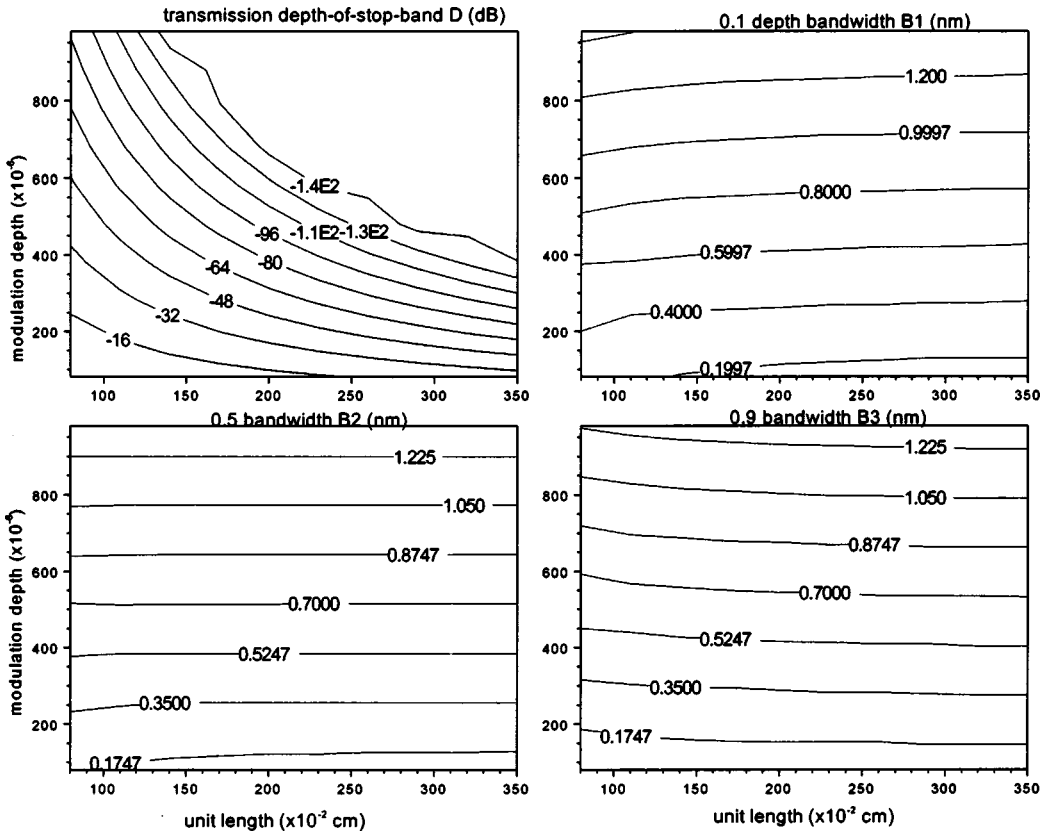

Fig. 4 The influence of the unit length L and the modulation depth δn on the feature parameter set stored in KB: top-left plot for D, top-right for $B1$, bottom-left for $B2$, and bottom-right for $B3$.

3 Learning Genetic Algorithm

3.1 *Learning Evolution*

Generally speaking, the LGA takes the target spectrum as the input and produces the calculated parameter set $(L, \Lambda, \delta n, \Delta\Lambda)$ as the output. Like all GA approaches,[11–14] an error function has to be defined first for performing evolution. Following Ref. 9, the expression in Eq. (5) is used as the criteria to determine which individual in the population is superior, so it has a larger probability for offspring.

$$Gi = \sum_{\lambda} [T_{t\,\mathrm{arg}\,et}(\lambda) - T_i(\lambda)]^2. \tag{5}$$

Throughout this work, the spectral coordinate is discretized into a dimension size of 512 grid points, and the summation in Eq. (5) is over all these grid points. The agenda of GA is to reduce the error between the target and the calculated transmission spectra, and the final best individual parameter set is generated as the solution. After each evolution, the decision procedure in the system decides whether the features of the newly calculated spectrum from the best individual parameter set are different enough when compared to the templates in the KB. If it is so, the parameter set will be stored in the KB. The LGA has two choices about expanding the KB: it can expand each time when the filter is evolved, or it can adjust the criteria for different situations. For example, when the LGA deals with almost similar spectra and high accuracy is required, then the LGA could decide to expand even when the difference between the evolved filter and the stored filters is not large. When the spectrum that is the same as one of the templates in KB is fed, the LGA outputs the parameter set directly. When the spectrum is similar to one of the templates in the KB, the LGA uses previous experiences to shorten the retrieving time as well as to increase the convergent correctness.

3.2 *Recognizing a Spectrum by Features*

The structure of the LGA is shown in Fig. 5. As an example, the spectrum in Fig. 1 is used as a target, and the

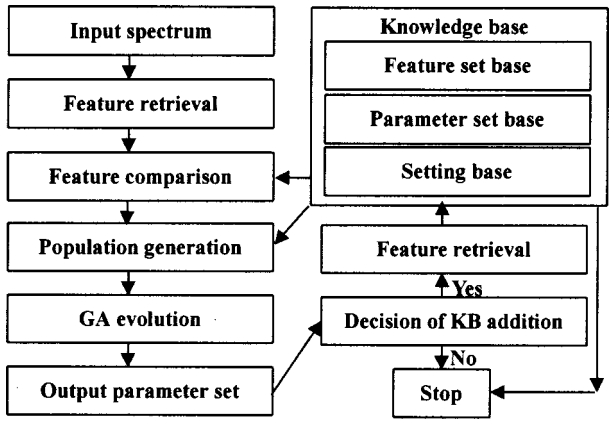

Fig. 5 The LGA flow chart.

Table 2 Feature set for the spectrum in Fig. 1.

Features	D	$B1$(nm)	$B2$(nm)	$B3$(nm)
Values	−47.77 dB	0.6156556	0.5467710	0.4778865

generated feature set by the retrieving procedure is shown in Table 2. Then the feature comparison procedure generates a similarity array that records the degree of similarity between the features of the input spectrum and those stored in the KB. The parameter set with the highest degree of similarity is fed to the population generation procedure to generate a suitable population for this spectrum. Random numbers in a suitable range stored in the setting base of the KB are generated to perturb the parameter set for forming other individuals in the initial population.

3.3 *Achievement by Feature Retrieving*

The overall speed of the whole design system depends on the weighting criteria for a special application. To demonstrate the advantages of using the KB, two systems that adopt the same error weighting, selection, mutation, and crossover rules are compared in the following tests. On our computer, when the feature and parameter base in the KB has the size of 100, the total time consumed for both feature retrieving and comparison has the value of 5 ms total for both population sizes of 6 and 75. The time required for generating a suitable population for the population size of 6 is about 3.7 s, and for the population size of 75 is 48.9 s. The comparison between the evolutions with and without KB is shown in Fig. 6. The dashed line represents the error convergence without the help of KB, and the solid line represents the case with KB. The time for one generation to evolve in this case is 3.0 s for the population size of 6, and 32.4 s for the population size of 75. For the evolution with the population size of 6 in Fig. 6(a), to get the error value in the range of 10^{-5} to 10^{-6}, the KB helps speed up the evolution by about 400 generations. Also as shown in Fig. 6(b), with the population size of 75, the KB can improve an unsatisfactory GA evolution to finally become an extremely accurate solution. Overall, the LGA greatly reduces the convergence error and the time consumed as compared to the previous work.[9] Because the time consumed for features comparison is much smaller than the time wasted without the KB, it may be advantageous to store a larger dimension of feature sets. When the relationship between the design parameters and the filter characteristics is known more completely, the KB can be expanded to include this knowledge.

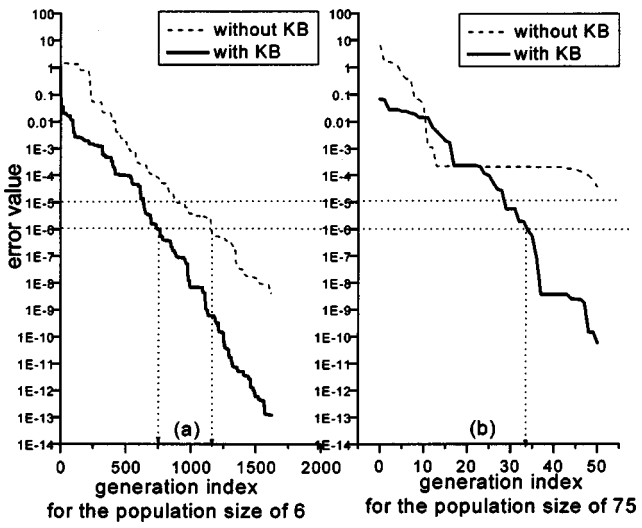

Fig. 6 Error comparison for cases with and without KB: (a) population size=6 and (b) population size=75.

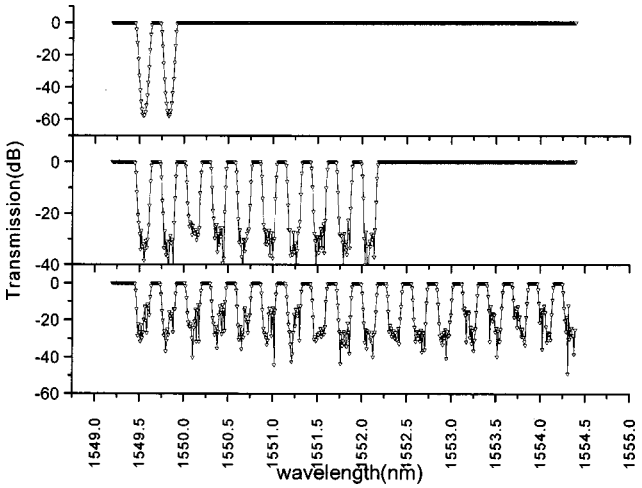

Fig. 7 Designed multiband FBG filters with 0.1-nm bandwidth and 0.28-nm channel spacing. The channel number=2, 10, and 20, respectively.

4 Design of Multiband FBG Transmission Filters

4.1 *Influence of the Channel Number*

As a practical design example, several multiband FBG transmission filters with 0.1-nm, 3-dB bandwidth, and 0.28-nm channel spacing and with different channel numbers have been designed by using the approach stated before. From the top to the bottom of Fig. 7, the numbers of stop bands are 2, 10, and 20, respectively. The case with two stop bands has a clean profile that is not influenced by the side bands of individual FBGs. The influence of the side bands of individual FBGs increases as the total number of stop bands increases. When the total number is 20, the transmission at some points of the stop bands can actually go beyond −20 dB. Table 3 shows the FBG parameters retrieved by the LGA.

4.2 *Influence of the Channel Spacing*

Transmission profiles with 20 stop bands and the same parameter set but with different $\Delta\Lambda$ are shown in Fig. 8. The pitch-period difference $\Delta\Lambda$ between each graph is 0.6 nm. The channel spacing of the designed filters are 0.67, 2.41,

Table 3 Parameter set for the spectrum in Fig. 7.

Parameters	L(cm)	Λ(nm)	δn	$\Delta\Lambda$(nm)
Retrieved	4.57	534	1.25×10^{-4}	0.0971

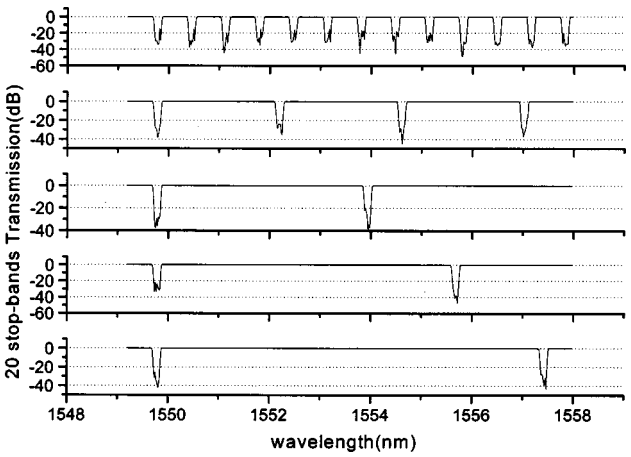

Fig. 8 Designed multiband FBG filters of 20 channels with channel spacing= 0.67, 2.41, 4.14, 5.87, and 7.6 nm, respectively.

4.14, 5.87, and 7.6 nm, respectively. It is found that the influence from the individual side bands decreases as the channel spacing increases. This clearly shows the tradeoff between the denser wavelength division multiplication channels and the lower transmission loss. In principle, it is possible to include in the evolutionary design the influence of the channel number and the channel spacing on the transmission stop-band loss. However, to save the computation time, it is normal to first design a profile with lower loss and with a lower number of stop bands. The required number of stop bands is then generated by cascading the period-shifted solutions.

5 Conclusion

An efficient approach for designing FBG filters in DWDM fiber communication systems is developed. The uniqueness of our method is the adoption of a KB in the initialization stage and a LGA tool in the design stage. When more and more examples of the FBG spectra and the corresponding design parameters are experienced, the LGA can automatically include the new knowledge like a learning expert. As a design expert, the LGA can also provide suggestions for the parameter range according to the given spectra, and evolve accurately to search the optimized parameter set by utilizing the learnt knowledge. This kind of FBG expert design system should be a handy tool for designing complicated FBG filters for different application purposes.

References

1. I. Ota, T. Tsuda, A. Shinozaki, S. Yodo, T. Ota, T. Shigematsu, and Y. Ibusuki, ''Development of optical fiber gratings for WDM systems,'' *Furukawa Rev.* **19**, 35–40 (2000).
2. S. V. Kartalopoulos, *DWDM Networks, Devices, and Technology*, John Wiley and Sons, NJ (2003).
3. R. Slavik and S. LaRochelle, ''Large band periodic filters for DWDM using multiple-superimposed fiber Bragg gratings,'' *IEEE Photonics Technol. Lett.* **14**(12), 1704–1706 (2002).
4. C. Yang and Y. Lai, ''Apodised fiber Bragg gratings fabricated with uniform phase mask using low cost apparatus,'' *Electron. Lett.* **36**(7), 655–657 (2000).
5. G. H. Song and S. Y. Shin, ''Design of corrugated waveguide filters by the Gel'fand-Levitan-Marchenko (GLM) inverse scattering method,'' *J. Opt. Soc. Am. A* **2**, 1905–1915 (1985).
6. E. Peral, J. Capmany, and J. Marti, ''Iterative solution to the Gel'fand-Levitan-Marchenko coupled equations and application,'' *IEEE J. Quantum Electron.* **32**, 2078–2084 (1996).
7. K. A. Winick and J. E. Roman, ''Design of corrugated waveguide filters by Fourier transform techniques,'' *IEEE J. Quantum Electron.* **26**, 1918–1929 (1990).
8. J. Skaar and K. M. Risvik, ''A genetic algorithm for the inverse problem in synthesis of fiber gratings,'' *J. Lightwave Technol.* **16**, 1928–1932 (1998).
9. G. Cormier and R. Boudreau, ''Real-coded genetic algoparameter synthesis,'' *J. Opt. Soc. Am. B* **18**(12), 1771–1776 (2001).
10. S. Huang, M. LeBlanc, M. M. Ohn, and R. M. Measures, ''Bragg intragrating structural sensing,'' *Appl. Opt.* **34**(22), 5003–5009 (1995).
11. X. Yao, *Evolutionary Computation—Theory and Application*, pp. 2–26, 235–255, World Scientific, Singapore (1999).
12. S. F. Shu, C. L. Pan, and C. T. Sun, ''Population-split genetic algorithm for retrieval of ultrafast laser parameters,'' *International Journal of Neural, Parallel & Scientific Computations* (in press).
13. S. F. Shu, and C. T. Sun, ''Object oriented probing technique for population split genetic algorithm activity in evolving laser parameters,'' (submitted for publication).
14. S. F. Shu, ''Controlling evolutionary path in laser parameter retrieval by a genetic algorithm with knowledge base,'' *Chinese Automatic Control Conf.*, pp. 578–582, R.O.C. Automatic Control Society, Tau-Yuan (2003).

Su-Frang Shu received the BS degree in electrical engineering in 1987 from National Chiao-Tung University (NCTU), Hsin-Chu, Taiwan. From 1987 to 1991, she was an assistant preacher studying Greek and the Bible. She received the MA degree in electro-optical engineering from the Institute of National Taiwan University, Taipei, in 1994. She was in charge of administration and design of a software network in the research center of Taiwan Taoyuan Hsin-Shing Professional High School from 1994 to 1999. She is currently an adjunct lecturer and assistant researcher with the Intelligent Behavior Laboratory at Chin-Yuan Technical College and is an optometry adjunct lecturer with the cooperation education of the National Open University and Shuw-rin Medicine School. As a PhD student in the Institute of Electro-Optical Engineering, NCTU, her research focuses on ultrafast lasers, optical fibers, computer science, biological theory, and their synthesis.

Yin-Chieh Lai is now a full professor at the Institute of Electro-Optical Engineering (IEO), National Chiao Tung University (NCTU), Taiwan. He got his PhD degree from MIT in 1991 and joined IEO/NCTU immediately after his graduation. From 1999 to 2001, he was on leave at the Opto-Electronics and Systems Laboratories (OES) at the Industrial Technology Research Institute (ITRI) in Taiwan as the director of the optical communication group for a period of two years. His research efforts are mainly in quantum theory of nonlinear optical pulse propagation, advanced fiber grating and all-fiber devices, modelocked Er-fiber lasers, new planar waveguide devices, and semiconductor microdisk and microring lasers.

Ci-Ling Pan is a professor with the Institute of Electro-Optical Engineering (IEO) and interim director of the Center of Excellence in Photonics Research, National Chiao Tung University (NCTU), Hsinchu, Taiwan. He received his PhD degree in physics from Colorado State University, Fort Collins, in 1979. He was the director of IEO, NCTU (1992 to 1995) and the coordinator of the photonics program of the National Science Council, Taiwan (1996 to 1999). His research interests are lasers and their applications in broadband optical communication, precision metrology, ultrafast optics, and optoelectronics. He is a member of the Physical Society and the Optical Engineering Society of China, IEEE, OSA, and SPIE. He was elected a member of the Phi Tau Phi Honor Society (1991) and a fellow of the Photonic Society of Chinese Americans (PSC) in 1998.